Materials and Structures (2009) 42:51–69
DOI 10.1617/s11527-008-9366-x

ORIGINAL ARTICLE

Plastic analysis of HSC beams in flexure

Luís F. A. Bernardo · Sérgio M. R. Lopes

Received: 9 November 2006 / Accepted: 26 February 2008 / Published online: 12 March 2008

Abstract This article presents an experimental study on the plastic behaviour of HSC beams in bending. Nineteen isostatic beams were tested up to failure. The loading consisted of two symmetrical concentrated forces applied approximately at thirds of the span of the beams. The main purpose of the analysis is to characterize the plastic rotation capacity in the beams' failure section with an experimental parameter. Bearing this in mind, a global plastic analysis of the tested beams is presented. The main variables of this study are the longitudinal tensile reinforcement ratio and the compressive strength of the concrete. The results obtained here are completed with others presented before and the whole set of results is analysed and discussed. The plastic rotation capacity of the tested beams are analysed with the rules of some codes of practice. Finally, a summary of the main conclusions is presented.

L. F. A. Bernardo (✉)
Departamento de Engenharia Civil e Arquitectura,
Universidade da Beira Interior, Edifício II das
Engenharias, Calçada Fonte do Lameiro, 6201-001
Covilha, Portugal
e-mail: luis.bernardo@ubi.pt

S. M. R. Lopes
Departamento de Engenharia Civil,
University of Coimbra, Coimbra, Portugal
e-mail: sergio@dec.uc.pt

Résumé *Ce travail décrit une etude expérimentale sur la capacité de rotation plastique de poutres en béton à haute résistance soumises à la flexion. Dix-neuf poutres isostatiques ont été testées jusqúà la rupture avec une charge constituée par deux forces concentrées et symétriques situées environ au tiers et aux deux tiers de la portée. L'objectif principal de l'analyse est de caractériser la capacité de rotation plastique de la section de rupture avec un paramètre de la tendance plastique. Pour ceci, une analyse plastique globale des poutres testées est présentée. La résistance du béton et le taux d'armatures longitudinales de traction constituent les variables principals de cette étude. Les résultats sont complétés avec ceux d'études précédentes et sont analysés et comparés. La capacité de rotation plastique des poutres est analysée faces aux règles de quelques codes importants aussi bien faces à certaines recommendations publiées. Finallement, un sommaire des principales conclusions est présenté.*

Keywords Plastic rotation capacity · Beams · High strength concrete · Reinforced concrete

1 Introduction

The evolution of chemical admixtures and minerals for the manufacturing of concrete has allowed the development of high performance concretes, characterized by vast improvements in terms of workability,

durability and mechanical resistance. High-strength concrete (HSC) becomes competitive in special structures compared to other structural materials. In the near future, the growing use of HSC in such structures will certainly result in a higher demand of this material.

In comparison to HSC, normal strength concrete (NSC) develops low levels of stresses but, in compensation, they are able to maintain that level during an appreciable interval of deformations. Is has been observed that the load carrying capacity of HSC is high, but after the peak load, it falls abruptly revealing a shape of the stress strain relationship quite different from that of NSC [12]. This behaviour clearly shows that HSC are more brittle than NSC.

The first observations of this high brittleness gave rise to some understandable doubts concerning the use of HSC in structures. The main point consisted of knowing if the structural elements made with this type of concrete would be sufficiently ductile. Due to this doubt, there has been a certain restriction in the use of HSC as structural material, mainly in constructions located in earthquake zones [25]. The use of HSC in structures located in these zones would depend on the existence of an appropriate inelastic deformability of the structural elements under cyclical loads such as those induced by an earthquake. A ductile behaviour would depend on the existence of an appropriate rotation capacity at the critical sections.

Fortunately, tests have shown that a small deformability in HSC does not necessarily result in fragile behaviour of structures made with this material. In fact, such a fragile behaviour can be controlled by an appropriate choice of the amount and location of the reinforcement bars in the design stage [32]. However, it should be taken into account that the detailing rules can differ from those adopted for NSC structures. For instance, when compared with NSC, the brittle behaviour observed in compression tests of HSC cubes or cylinders, which is reflected in the stress–strain relationships, would lead to changes in some clauses presented by codes of practice for NSC, such those related with minimum flexural ductility (limit values for the amount of reinforcement or for the x/d parameter). For instance, as explained later in this paper, the limit of x/d would allow for higher amounts of steel in HSC beams.

The rotation capacity in the element's critical sections is directly related with the ductility of that element. Nowadays, the ductility of structures is considered of the utmost importance, because it is directly related with the structural safety and also with the redistribution capacity of internal forces.

In order to ensure enough ductility, all the structural elements should be correctly reinforced: the detailed rules created for that purpose, especially in codes of practice, should be respected. Besides, the ductility of the structural elements depends directly on the plastic rotation capacity of the critical sections obtained through:

- The choice of suitable ductility characteristics of steel;
- The design of the section so that the relative height of the compressed concrete in failure, defined through parameter x/d is small (x—depth of neutral axis, d—effective depth);
- The adoption of transversal reinforcement with spacings sufficiently small to guarantee a suitable confinement of the compressed concrete.

The redistribution of moments depends on the existence of an appropriate ductility in the areas designated by plastic hinges (areas where the longitudinal reinforcements are plasticized). Once a plastic hinge is created at a certain location, other sections still withstand further moments, and internal redistributions of forces cause more plastic hinges to be sequentially formed, up to the creation of a mechanism. This process wills guarantee that more sections will get to reach its full resistance, rather than just one.

The rotation capacity of HSC structures is a very important issue, which should be fully known in order to allow the safe use of this material in structures.

The work presented here consists of an experimental study carried out in order to analyse the plastic rotation capacity in HSC beams subjected to pure bending in the failure zone. This work also constitutes the extension of an earlier study accomplished by the authors and already published (Lopes and Bernardo [17]). For this purpose a set of new beams, with similar geometry and different concrete strengths, were tested in order to increase the available results for more consistent conclusions. In this paper the authors want also to check if the practical rule of limiting the relative height of the compressed concrete in failure (in critical sections)

and the amount of reinforcement, rule accepted and used nowadays for NSC, is also valid for HSC beams.

2 Previous studies

In contrast with the apparent brittleness observed in the HSC test cylinders or cubes, the first experimental work on the ductility in HSC beams, accomplished by Leslie et al. [16], did not show a brittle behaviour for these beams. Further experimental studies, such as that by Shah and Ahmad [25], indicate that the ductility of the structural elements made with HSC was acceptable for seismic resistance as long as certain limits for key parameters would be respected. As in NSC, one of the most important parameters is the longitudinal tensile reinforcement ratio of the beams.

The study carried out by Leslie et al. [16] showed the influence of some parameters in the ductility of HSC beams subjected to pure bending in the critical zone, namely the compressive strength of the concrete and the percentage of longitudinal tensile reinforcement. Later, further studies confirmed the general influence of the percentage of longitudinal compression reinforcement and the percentage of transverse reinforcement. Among those studies, some deserve attention, namely Tognon et al. [34], Pastor et al. [21], Naaman et al. [19], Shin [27], Shin et al. [28, 29], Hansen and Tomaszewicz [13], Ahmad and Barker [3], Shehata and Shehata [26], Pam et al. [20], Bernardo and Lopes [4], Lopes and Bernardo [17] and Carmo and Lopes [6].

In spite of the number of referred works in the previous section, some doubts still persist, for instance, the exact influence of the strength of the concrete on the flexural ductility is not clear. Some works [6, 17, 20, 21, 29, 34] indicate that the ductility in beams increases as the compressive strength of the concrete increases. The studies made by the authors [4, 17] were especially focused on this problem, and the referred tendency was observed for concrete compressive strength above 60 MPa. Other works [2, 16] indicate the opposite. As far as the longitudinal tensile reinforcement ratio is concerned, there is a consensus among all of the referred studies that indicates that the ductility decreases with an increase in this ratio. However, the interval of appropriate values for the amount of longitudinal tensile reinforcement is still under controversy.

Bernardo and Lopes [5] have studied the influence of the depth of the compression zone on the failure and on the ductility of beams under flexure. They have used ductility indexes and they have observed a general trend on the behavior of HSC beams that is similar to that of NSC: the ductility increases as the depth of the neutral axis decreases. However limits for the limitation of x/d are not yet recommended. The validity of the current x/d values of codes of practice were not checked either.

Recently, the ductility of HSC beams was indirectly studied by means of the plastic rotation capacity of the critical section (Pecce and Fabbrocino [23], Ko et al. [14], Lopes and Bernardo [17] and CEB No. 242 [8]). This property is related with the ductility and, therefore the results obtained with ductility indexes can be confirmed.

The studies on this subject are still continuing in some research units. The recent findings were important to open up the range of concrete strength that the design rules of codes of practice apply. In fact, the last versions of the codes worldwide have incorporated clauses on ductility for HSC. For instance, recommendations of ACI Committee 363 [2] and CEB [7] helped to introduce changes in that direction. Published recommendations by Taerwe [33] for the European code, by Rangan [24] for the ACI code, Paultre and Mitchell [22] in an international perspective and Mendis [18] are examples of further proposals for changing the codes rules. Such recommendations are not fully incorporated into the codes. Since some aspects of the structural behaviour of HSC beams do not have an overall acceptance from the scientific community, especially concerning the establishment of codes rules to ensure a ductile behaviour of members under flexure, further experimental and theoretical studies need to be carried out.

Some experimental programmes should be carried out to study the ductility of the HSC beams and the parameters that influence it. Once the ductility is directly related to the rotation capacity in the critical zones, this property is of the utmost importance.

Some authors have already studied the service behaviour of HSC structural members, namely cracking and deformation (for instance, Lambotte and Taerwe [15]).

3 Research significance

The non-linear behaviour of NSC is normally taken into account in codes of practice worldwide. For hyperstatic structures, coefficients of redistribution are defined to change the maximum negative moments calculated by linear elastic analysis. However, apart from recent updated European code EC 2 [10], generally, codes do not give guidance on this for HSC structures. Knowledge of how the plastic rotation capacity varies in HSC beams its useful, so that the designer knows if the failure of the critical sections is ductile or brittle. The amount of experimental work analysed here covers a large range of current cases and gives good indications on the behaviour of HSC beams.

The majority of the published studies on ductility of HSC beams use ductility indexes based on deformation values as the main comparison parameters. When the main purpose is to analyse the plastic rotation capacity (which is related with the ductility of the beams), the use of the ductility indexes is not adequate, and other approach needs to be considered. In this article, and in line with other paper published by the authors where they presented an original approach [17], a new parameter called PTP was used by the authors. This parameter produces a direct characterization of the plastic rotation capacity of HSC beams. The conclusions obtained with this parameter can, therefore, be compared with other studies where ductility indexes were used as the main parameter.

4 Description of the experimental program

The experimental program presented here consisted of 19 main tests of simply supported beams up to failure. As already described by the authors [17], the beams were tested by means of two point loads symmetrically located approximately at thirds span. This type of loading was chosen to obtain a central region under pure bending (without the influence of shear). The beams were 3.00 m long, with a rectangular cross section in general of 0.12 × 0.27 m. The failure of the beams always occurred through bending in the area between the applied forces.

Figure 1 gives a schematic representation of the geometrical characteristics and the details of reinforcements adopted for the experimental models. As the longitudinal tensile reinforcement ratio is one of the variables studied here, it is not shown in Fig. 1, and will be presented later. With the purpose of preventing failure by shear in the region close to the supports, a transverse reinforcement constituted by closely spaced stirrups was provided in these zones. One of the purposes of this work was to study the failure in simple bending, without confinement of the compressed concrete. Consequently, the central area subjected to pure bending did not have transverse reinforcements (stirrups).

Table 1 presents the solutions used for the longitudinal tensile reinforcement of the beams. Hot-rolled steel ribbed bars were used for the longitudinal tensile reinforcement. A top reinforcement formed by two 6 mm diameter longitudinal bars was also used only for constructive reasons.

Table 2 summarizes the geometrical and mechanical characteristics of each test beam, namely the width (b) and the height (h) of the cross-section, the effective depth (d), the area of longitudinal tensile reinforcement (A_s) and the reinforcement ratios ρ and ρ_b (longitudinal tensile reinforcement ratio that theoretically leads to the so-called balanced condition for the strains, as defined in ACI Code) as well as the ratio (ρ/ρ_b), the average compressive strength of the concrete (f_c) and the elasticity modulus (E_c). The modulus of elasticity of the concrete, E_c, was computed according to the equation proposed by Taerwe [33] for the HSC. Table 2 also presents the characteristics of the beams previously tested by the authors [17]. Finally, Table 2 also presents, for all

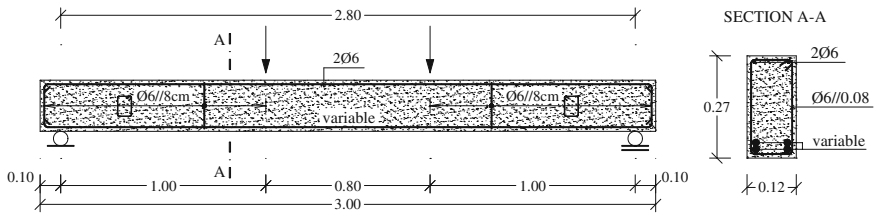

Fig. 1 Geometry and details of tested beams

Table 1 Tension reinforcement of test specimens

SECTION TYPE	1	2	3	4	5
DETAILING	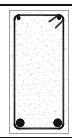	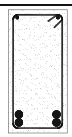		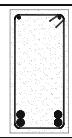	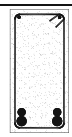
BARS	**2 16**	**4 12**	**2 16+2 12**	**4 16**	**2 20+2 16**
AREA (cm^2)	**4.02**	**4.52**	**6.28**	**8.04**	**10.30**

Table 2 Geometrical and mechanical beam properties

Beam	B (mm)	H (mm)	D (mm)	A_s (cm^2)	ρ^a (%)	$\rho_b{}^b$ (%)	ρ/ρ_b (−)	f_c (MPa)	$E_c{}^c$ (GPa)	Mix design
A(62.9-1.52) [17]	125	270	238	4.52	1.52	3.44	0.44	62.9	39.59	[d]
A(64.9-2.04) [17]	130	270	237	6.28	2.04	3.36	0.61	64.9	39.93	[d]
A(64.1-2.21) [17]	120	270	237	6.28	2.21	3.32	0.67	64.1	39.80	[d]
A(63.2-2.86) [17]	120	270	234	8.04	2.86	3.10	0.92	63.2	39.64	[d]
A(65.1-2.86) [17]	120	270	234	8.04	2.86	3.19	0.90	65.1	39.96	[d]
B(79.2-1.59)	120	264	237	4.52	1.59	4.33	0.37	79.2	42.13	2
B(78.9-2.09)	124	270	242	6.28	2.09	4.08	0.51	78.9	42.09	2
B(78.5-2.16)	120	270	242	6.28	2.16	4.06	0.53	78.5	42.03	1
C(82.9-2.11) [17]	123	270	242	6.28	2.11	4.29	0.49	82.9	42.65	3
C(83.9-2.16) [17]	120	270	242	6.28	2.16	4.34	0.50	83.9	42.79	2
C(83.6-2.69) [17]	125	270	239	8.04	2.69	4.10	0.66	83.6	42.75	3
C(83.4-2.70) [17]	122	275	244	8.04	2.70	4.09	0.66	83.4	42.73	2
D(88.0-1.36)	120	270	247	4.02	1.36	4.32	0.31	88.0	43.37	1
D(85.8-3.61)	120	270	238	10.30	3.61	4.22	0.86	85.8	43.06	3
D(86.0-3.61)	120	270	238	10.30	3.61	4.23	0.85	86.0	43.09	3
E(94.6-2.73)	123	270	239	8.04	2.73	4.64	0.59	94.6	44.23	1
E(90.2-2.80)	120	270	239	8.04	2.80	4.42	0.63	90.2	43.66	2
F(100.3-1.96)	139	263	230	6.28	1.96	5.19	0.38	100.3	44.95	3
F(105.2-2.66)	129	270	234	8.04	2.66	5.16	0.52	105.2	45.55	3

[a] $\rho = A_s/bd$

[b] $\rho_b = (0.85 \times 0.65 f_c/f_y) \times [87{,}000/(87{,}000 + f_y)]$ [1]

[c] $E_c = 22[(f_{ck} + 8)/10]^{0.3}$ (f_{ck} in MPa) [33]

[d] The concrete was supplied commercially

test beams, the type of mix design used to produce the concrete and the details of each mix are presented in Table 3.

In order to simplify the analysis of the results, the experimental models are grouped in 6 series (A, B, C, D, E and F), according to the resistance ranges obtained for the concretes. The type of labelling of the beam was chosen in order to give important information for this type of study (see Table 2). Each series (A–F) is presented along with the compressive strength of the concrete, f_c, (first number) and to the longitudinal tensile reinforcement ratio, ρ (second number).

The compressive strength of the concrete was determined by compression tests on typical samples of each mix of concrete.

In order to evaluate the strains and stresses corresponding to the initiation of yielding in the reinforcements bars, steel samples were also tested in tension [17].

Figure 2 shows a schematic representation of the experimental models as they were tested, and also the

Table 3 Mix design

Component	Mix design (content per cubic meter)		
	1	2	3
Natural sand (kg)	448.50	375.00	417.00
Crushed aggregates			
Granite D_{max} = 19.1 mm (kg)	–	1245.00	1240.00
Limestone D_{max} = 12.5 mm (kg)	1145.70	–	–
Normal Portland cement type I/42.5R (kg)	475.00	525.00	525.00
Admixture			
Sikament 163 (l)	–	1.30	1.30
Sikament FF (l)	11.90	15.75	–
Rheobuild 1000 (l)	–	–	10.50
Silica Fume Sikacrete HD (kg)	–	–	55.00
Fly ash (kg)	53.00	55.00	–
Water (l)	185.00	155.00	145.00
Ratio W/(C + Additive)	0.35	0.27	0.25
Volumetric mass (kg/m^3)	2321.80	2375.00	2396.00

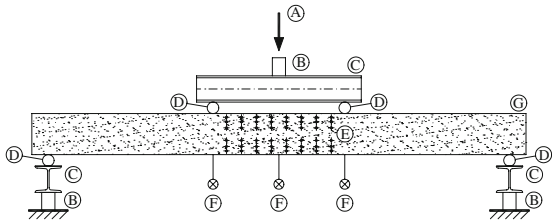

Fig. 2 Typical set-up for testing beam specimen. A—applied load, B—load cell, C—steel beam, D—roller support, E—Demecs, F—displacement transducer, G—beam test

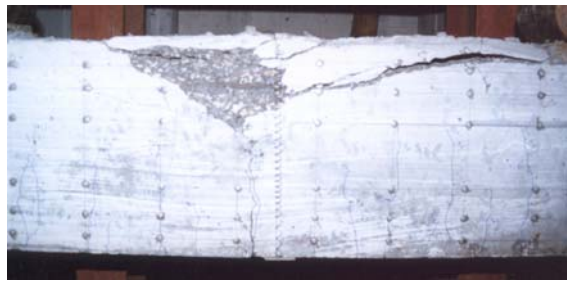

Fig. 3 Typical beam after failure

external measurement instruments and the spreader beam used to divide the jack force into two point loads. The main load was applied through an electromechanical actuator applied by means of a rigid steel test frame. The total value of the applied load was measured, continuously, by means of strategically located load cells (see Fig. 2). The vertical displacements were measured through displacement transducers placed at mid span of the beams and also underneath both sections where the point loads were applied. The strains were also measured along the height of the beams in the central area (between the point loads). For this purpose, an external grid of Demec measuring points was stuck to the lateral faces of the beams (Fig. 2). Resistance strain gauges were fixed to the longitudinal tensile reinforcement in the mid span area to measure the evolution of strains of the steel bars during the test. All the readings from the measuring instruments were recorded on a data logger acquisition equipment.

All the tests were performed under displacement control. This procedure was useful for the study of beams after the maximum peak load.

Figure 3 shows a close up of a beam after failure, which occurred (by bending) in the central area. Such failure type was typical for the whole set of test beams.

5 Analysis of the experimental results and discussion

5.1 Rotations and deflection

Figures 5–10 presents the experimental Rotation (θ)–Deflection at mid span (δ) curves for each series of

beams. The figures also include results from previous tests conducted by the authors [17]. Each graph shows the experimental and theoretical curves. The theoretical curves were obtained by using a theoretical elastic analysis (TEA) with homogenized section (taking into account the reinforcement of the cross section) and a theoretical plastic analysis (TPA) of the beams (assuming a mechanism for the beam).

The theoretical values of the rotations and deflections in plastic behaviour were obtained by assuming a mechanism created by a plastic hinge located at mid span [17]. In fact, it was experimentally observed that the plasticized zone of the beams always occured at mid span; hence the location of the plastic hinge should follow this rule.

The values of the elastic curvatures were calculated using the strain diagrams, assuming a state of pure bending. The theoretical values of the elastic rotations were obtained by multiplying the elastic curvatures by a length of 0.10 m corresponding to the distance between each pair of Demecs (Fig. 4). The value assumed for the distance between pairs of Demecs (0.10 m) would be confirmed later. The theoretical values of δ at mid-span in elastic behaviour were computed with the concrete modulus of elasticity presented in Table 2.

The experimental points of the curves θ–δ were obtained directly from the tests. The experimental rotations, θ, represent the relative rotation between the two sections coincident to the location of vertical line Demec points. Since the Demec grid comprised eight vertical lines, the two chosen neighbouring columns were those between which failure took place. The rotations are obtained by multiplying the experimental values of curvatures by 0.10 m (Fig. 4), to maintain the same procedure followed before, for the elastic theoretical behaviour. It should be pointed out that the values of the experimental rotations were obtained through readings over a length of 0.10 m and an elastic part might be included together with the plastic part.

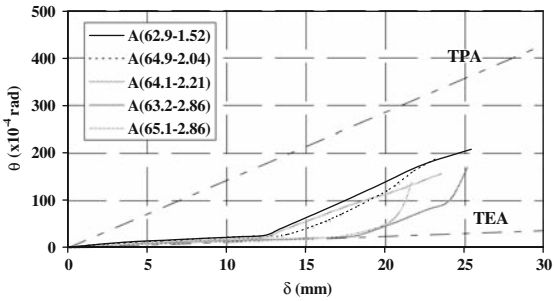

Fig. 5 Rotation–deflection curves (Series A [17])

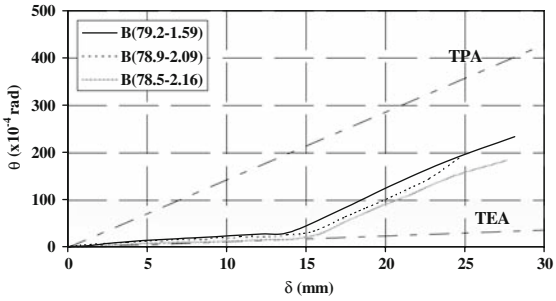

Fig. 6 Rotation–deflection curves (Series B)

Observing Figs. 5–10, it is clear that all beams have shown an almost perfect elastic behaviour during a relatively long initial phase of the tests. The point where the experimental values shift from the linear response corresponds to the initiation of yielding in the steel bars. Before this point, even the cracking of the concrete is not clearly visible on the graphs, even upon zooming in on the initial part of the graph.

When the longitudinal tensile bars start yielding, the experimental rotations abruptly increase, adopting a new slope comparable to that of the straight line of the theoretical plastic analysis (TPA). Therefore, immediately after yielding of the steel, the rotations of the beams follow the calculated rotations from the plastic model. Furthermore, the results being so close to the plastic behaviour, the reading length of 0.10 m

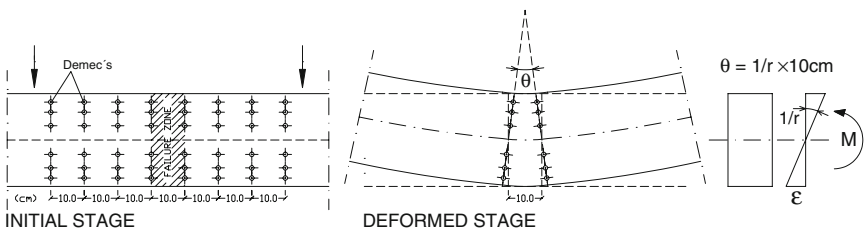

Fig. 4 Methodology to calculate the rotations

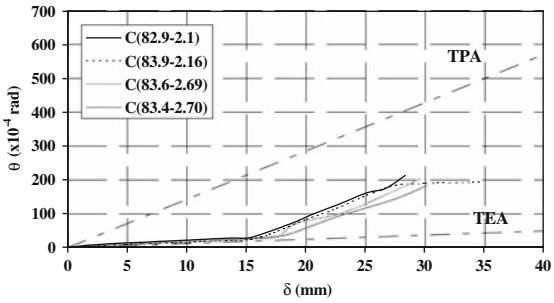

Fig. 7 Rotation–deflection curves (Series C [17])

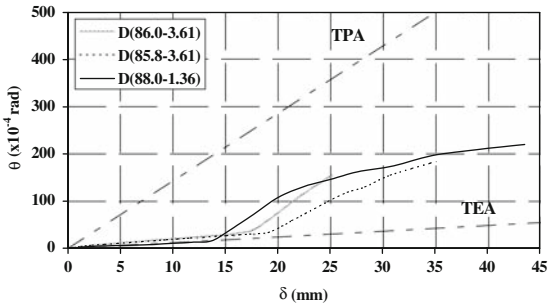

Fig. 8 Rotation–deflection curves (Series D)

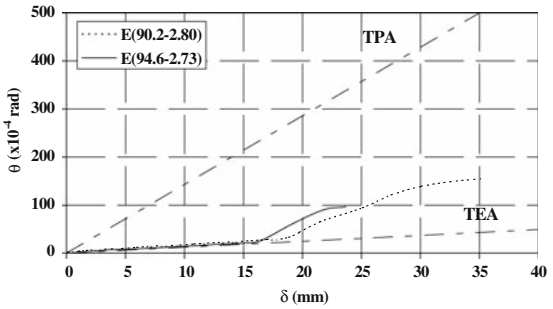

Fig. 9 Rotation–deflection curves (Series E)

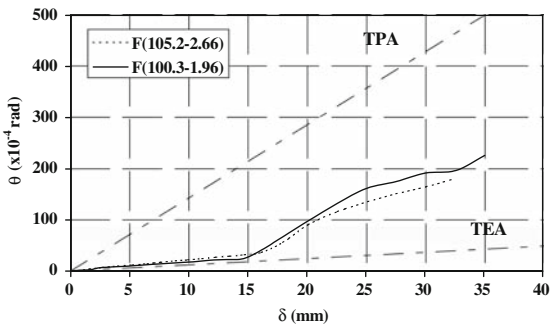

Fig. 10 Rotation–deflection curves (Series F)

for the strains seems to be perfectly valid as far as evaluating the rotations is concerned. Since the evolution of the plastic rotations of the test beams are very close to the theoretical predictions obtained from the plastic theory analysis (the experimental and the theoretical curves are approximately parallel), then it may be accepted that a plastic hinge was formed and that the length of this hinge is approximately equal to the distance between the vertical lines of demecs (100 mm).

All the previous observations are in agreement with those made by the authors in their earlier study with only nine tested beams [17].

5.2 Study of the plastic rotation capacity

5.2.1 Experimental evaluation of the plastic rotation capacity

The analyses of the experimental data presented in this section aims at highlighting the plastic behaviour of the tested beams. In order to have a quantitative value for comparison purposes, the authors previously defined a parameter that could evaluate the capacity of plastic rotation of a beam [17]. In the next paragraphs, a summary of the methodology used by the authors for the computation of that parameter is presented. A more detailed explanation can be found in [17].

As explained before, the experimental values of the relative rotations between the sections in failure area (sections with the vertical lines of Demec points) include the elastic and plastic part of the rotation. To study only the plastic part of the rotation it is necessary to eliminate the elastic part of the recorded experimental values. For each beam, and for each load step, the elastic portion was computed considering an elastic behaviour in non-cracked stage and cracked stage (until yielding of the reinforcement). The plastic portion was obtained by subtracting the theoretical elastic portion from the total value read during the tests. This calculation procedure is valid, since, for low levels of loading the predicted theoretical values agreed with the values from the tests (see Figs. 5–10). Consequently, the experimental graphs θ_p–δ (where the parameter θ_p represents the experimental plastic rotation) were plotted and presented in Figs. 11–16. These graphs are grouped in series of beams, and the axes are non-dimensional

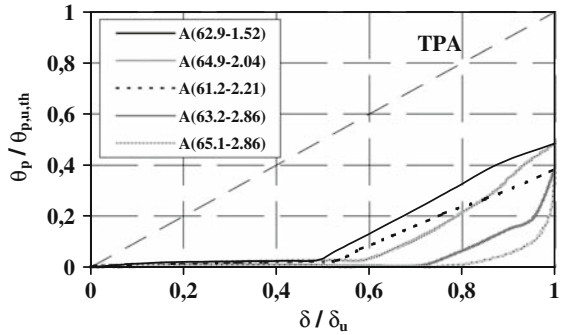

Fig. 11 Plastic rotation–deflection curves (Series A [17])

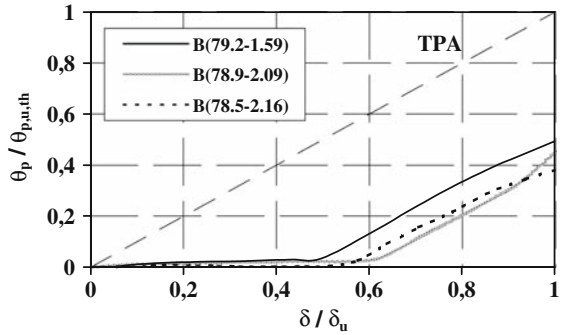

Fig. 12 Plastic Rotation–deflection curves (Series B)

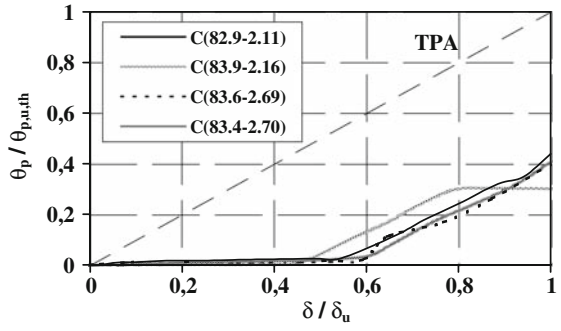

Fig. 13 Plastic rotation–deflection curves (Series C [17])

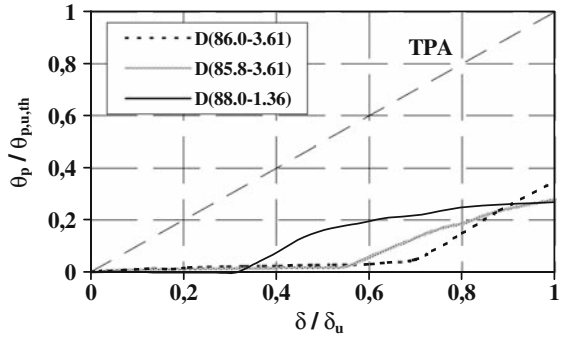

Fig. 14 Plastic rotation–deflection curves (Series D)

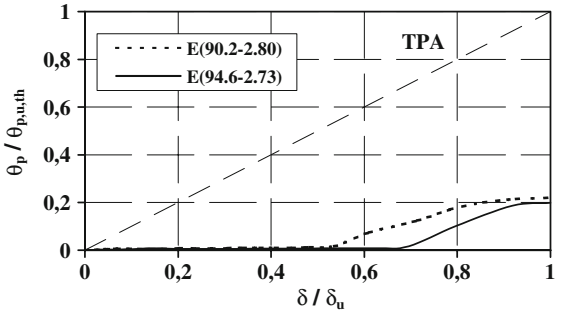

Fig. 15 Plastic rotation–deflection curves (Series E)

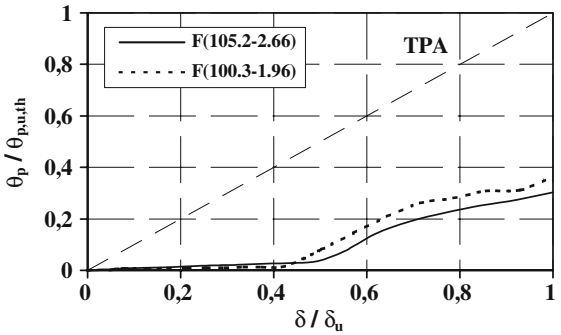

Fig. 16 Plastic rotation–deflection curves (Series F)

for a better interpretation and comparison purposes. The graphs of Figs. 11–16 also include the beams previously tested by the authors [17]. The meaning of the parameters is as follows:

- θ_p: Experimental plastic rotation;
- $\theta_{p,u,th}$: Ultimate value of the plastic rotation in theoretical plastic behaviour, corresponding to the ultimate experimental value of the deflection (δ_u);
- δ: Experimental deflection at mid span;
- δ_u: Ultimate value of the measured deflection (maximum deflection at the end of the test).

Two parameters, $C_{p,ex}$ and $C_{p,th}$, computed from Figs. 11–16, represent the area between the experimental curve ($C_{p,ex}$) and by the line corresponding to the theoretical analysis in plastic behaviour ($C_{p,th}$), respectively. From the graphs in Figs. 11–16, the value of the parameter $C_{p,th}$ is constant and equal to 0.5. The ratio $C_{p,ex}/C_{p,th}$ is designated by Plastic Trend Parameter (PTP) and gives an indication of the actual degree of the plastic rotation capacity compared with the theoretical perfectly plastic behaviour. Therefore, the higher the value of the PTP parameter

the larger the experiment plastic rotation capacity for one tested beam. The values obtained for the PTP parameter are indicated in Table 4.

5.2.2 *Study of the concrete strength on the plastic rotation capacity*

Table 4 groups the test beams according to its longitudinal reinforcement ratio (ρ and ρ_b) and presents, for each series of the beams, the average value for the longitudinal tensile reinforcement ratios (ρ_m) and for ρ/ρ_b ratios ($(\rho/\rho_b)_m$). It also presents the PTP parameter and the results concerning the beams previously tested by the authors [17].

The influence of concrete strength on the plastic rotation capacity can be analysed for series II and III (series with a larger number of beams). Figures 17, 18 show the corresponding graphs, where the beams tested in this work are presented by filled circles, and the beams of the reference [17] are presented by empty circles. A linear regression line was added to the graph to better visualize the general trend. In Fig. 18 the point of the graph corresponding to Beam E(94.6-2.73) was not drawn, because it had a non explained premature failure. This was observed during the tests and the results of PTP are quite different from those of the similar Beam E(90.2-2.80) (see Table 4).

From Figs. 17, 18, a general tendency for a small increase of the plastic rotation capacity as the concrete strength increases is observed. Such tendency is in agreement with previous results of the authors with a smaller number of beams [17]. Such an increase seems to be larger as the longitudinal tensile reinforcement ratio increases (see equations of the linear regression lines). This influence of the concrete strength on the plastic rotation can be explained through the position of the neutral axis: maintaining the same longitudinal tensile reinforcement ratio, the depth of the neutral axis at failure decreases as the concrete strength increases. In consequence, the failure becomes more ductile. Therefore, as a logical deduction, the depth of the neutral axis appears to have more influence on the rotational capacity of the beam than the loss of ductility of the material itself. Therefore, an appropriate use of HSC and steel reinforcement can eliminate the apparent more fragility of this type of concrete when compared with NSC.

These tendencies confirm the results obtained by other authors [4, 17, 21, 29, 34] as far as the influence

Table 4 Beam series with similar longitudinal reinforcement

Series	Beam	ρ (%)	ρ_m (%)	ρ_b (%)	ρ/ρ_b	$(\rho/\rho_b)_m$	f_c (MPa)	PTP (%)
I	A(62.9-1.52) [17]	1.52	1.49	3.44	0.44	0.37	62.9	29.10
	B(79.2-1.59)	1.59		4.33	0.37		79.2	29.54
	D(88.0-1.36)	1.36		4.32	0.31		88.0	25.68
II	A(64.1-2.21) [17]	2.21	2.10	3.32	0.67	0.53	64.1	21.08
	A(64.9-2.04) [17]	2.04		3.36	0.61		64.9	20.96
	B(78.5-2.16)	2.16		4.06	0.53		78.5	19.18
	B(78.9-2.09)	2.09		4.08	0.51		78.9	18.88
	C(82.9-2.11) [17]	2.11		4.29	0.49		82.9	21.52
	C(83.9-2.16) [17]	2.16		4.34	0.50		83.9	23.66
	F(100.3-1.96)	1.96		5.19	0.38		100.3	26.32
III	A(63.2-2.86) [17]	2.86	2.76	3.10	0.92	0.70	63.2	8.24
	A(65.1-2.86) [17]	2.86		3.19	0.90		65.1	4.12
	C(83.4-2.70) [17]	2.70		4.09	0.66		83.4	19.36
	C(83.6-2.69) [17]	2.69		4.10	0.66		83.6	18.56
	E(90.2-2.80)	2.80		4.42	0.63		90.2	14.36
	E(94.6-2.73)	2.73		4.64	0.59		94.6	8.76
	F(105.2-2.66)	2.66		5.16	0.52		105.2	21.58
IV	D(85.8-3.61)	3.61	3.61	4.22	0.86	0.86	85.8	16.42
	D(86.0-3.61)	3.61		4.23	0.85		86.0	14.84

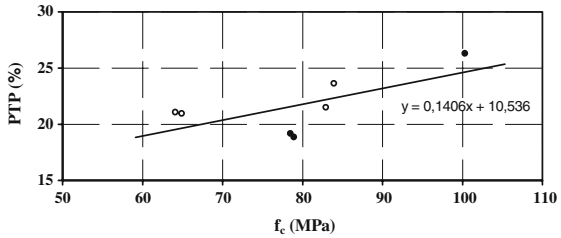

Fig. 17 Influence of concrete strength on plastic rotation capacity (Series II: $\rho_m = 2.10\%$; $(\rho/\rho_b)_m = 0.53$)

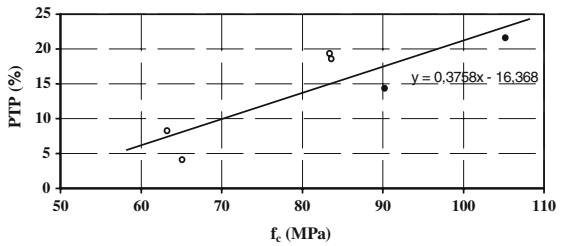

Fig. 18 Influence of concrete strength on plastic rotation capacity (Series III: $\rho_m = 2.76\%$; $(\rho/\rho_b)_m = 0.70$)

of concrete strength on the flexural ductility of HSC beams is concerned. Obviously, if the rotation capacity increases then the ductility also increases, because such properties are related with each other. The conclusions of this work are, however, in contradiction with those obtained by some other authors [3, 26].

5.2.3 *Influence of the reinforcement on the plastic rotation capacity*

Table 5 groups the beams by concrete strengths and presents, for each series of beams, the average value for the strength of the concrete ($f_{c,m}$) and it includes, like in Table 4, the beams of reference [17]. Since these beams have different concrete strengths, two new series are added to the table.

The evolution of the PTP parameter with the longitudinal tensile reinforcement ratio can be observed in Figs. 19, 20. The graphs include the results obtained for the whole set of test beams, including the beams from reference [17], independently of concrete strength (as observed in Figs. 17, 18, this parameter has little influence on plastic behaviour). A distinction was also made between the beams of this work and those from reference [17] (as in Figs. 17, 18). The graphs also include exponential tendency curves that seem to adjust to the results in a

Table 5 Beam series with similar concrete strength

Series	Beam	f_c (MPa)	$f_{c,m}$ (MPa)	ρ (%)	ρ_b (%)	ρ/ρ_b	PTP (%)
I	A(62.9-1.52) [17]	62.9	64.0	1.52	3.44	0.44	29.10
	A(64.9-2.04) [17]	64.9		2.04	3.36	0.61	20.96
	A(64.1-2.21) [17]	64.1		2.21	3.32	0.67	21.08
	A(63.2-2.86) [17]	63.2		2.86	3.10	0.92	8.24
	A(65.1-2.86) [17]	65.1		2.86	3.19	0.90	4.12
II	B(79.2-1.59)	79.2	78.9	1.59	4.33	0.37	29.54
	B(78.9-2.09)	78.9		2.09	4.08	0.51	18.88
	B(78.5-2.16)	78.5		2.16	4.06	0.53	19.18
III	C(82.9-2.11) [17]	82.9	83.5	2.11	4.29	0.49	21.52
	C(83.9-2.16) [17]	83.9		2.16	4.34	0.50	23.66
	C(83.6-2.69) [17]	83.6		2.69	4.10	0.66	18.56
	C(83.4-2.70) [17]	83.4		2.70	4.09	0.66	19.36
IV	D(88.0-1.36)	88.0	86.6	1.36	4.32	0.31	25.68
	D(85.8-3.61)	85.8		3.61	4.22	0.86	16.42
	D(86.0-3.61)	86.0		3.61	4.23	0.85	14.84
V	E(94.6-2.73)	94.6	92.4	2.73	4.64	0.59	8.76
	E(90.2-2.80)	90.2		2.80	4.42	0.63	14.36
VI	F(100.3-1.96)	100.3	102.8	1.96	5.19	0.38	26.32
	F(105.2-2.66)	105.2		2.66	5.16	0.52	21.58

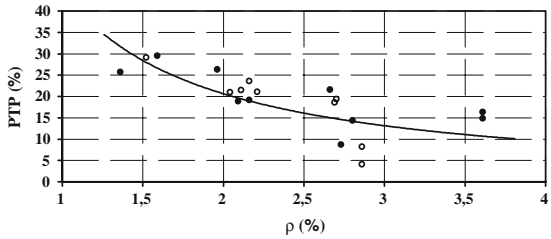

Fig. 19 Influence of longitudinal reinforcement ratio on plastic rotation capacity

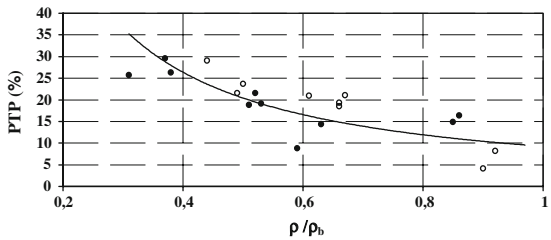

Fig. 20 Influence of ratio ρ/ρ_b on plastic rotation capacity

better way than straight lines, as previously used by the authors with a smaller number of beams [17].

The analysis of Figs. 19, 20 shows a reduction of the plastic rotation capacity as the longitudinal reinforcement ratio increases up to values of approximately $\rho \approx 3.0\%$ and $\rho/\rho_b \approx 0.7$. Beyond these values, the graphs suggest that the plastic rotation capacity tends to constant values, independent of the amount of longitudinal tensile reinforcement.

By comparing the results obtained with those of the previous section, the longitudinal tensile reinforcement ratio is definitely the most influencing parameter as far as the plastic rotation capacity (and, therefore, the ductility) is concerned. Such conclusions was also defended by other authors [4, 16, 17, 21, 25, 26, 34].

6 Comparison of experimental results to codes provisions

6.1 Flexural ductility in beams

As far as simple bending is concerned, the code provisions essentially focuses on the limitation of the percentage of longitudinal steel reinforcement and the relative height of the compressed concrete area at failure. This section aims to compare code provisions with the results from the tests. Some codes provide design rules which limit the ductility of the structures to some minimum levels. Recently, to the codes were made some changes in order to extend the validation of some practical rules to HSC. The comparative study is carried out by using the test results from the experimental programme and by using the PTP parameter for a plastic analysis of the test beams. European Code (MC 90 [9]), American Code (ACI 318 [1]) and Canadian Code (A23.3-04 [11]) are included in this analysis because they are important in terms of the countries that are covered. Although MC 90 is not a legal code, it had a great influence on the European Code (EC 2 [10]) which is applied in a great number of European countries. Being, most of the times, ahead of the European Code, it makes sense to use it in research work.

Only the codes rules related to the maximum values for the longitudinal reinforcement and for the relative depth of the neutral axis x/d are analysed here (x = depth of the neutral axis and d = effective depth of the section).

By fixing a maximum value for the reinforcement steel it is possible to avoid high concentration of bars. This fact presents construction advantages as well as better ductility behaviour of the structure. However, the upper limit of the reinforcement steel is typically very simple (for instance, indicating a maximum percentage of 4% of the concrete area) instead of a more elaborated approach (considering the mechanical properties of the cross section).

As far as x/d parameter is concerned, the codes requirements have some differences depending on the type of analysis that is to be implemented. For a linear analysis followed by limited redistribution of the moments, the x/d value will depend on the degree of redistribution intended by the designer (within the code limits). For a plastic analysis, the limit value for x/d is smaller than the limit requested for the previously referred analysis. Normally, the codes present a limitation for the maximum value of x/d parameter in order to ensure minimum ductility and some reserve of rotation capacity for the plastic hinges zones. The aim is that yielding of the steel bars occurs before the crushing of the concrete. This limitation will be used in the next sections of this paper, because it is very easy to be used in conjunction with a linear elastic analysis.

6.2 Code provisions and proposals for HSC beams

6.2.1 European Code MC 90 (1990)

In the absence of a specific study, the commentary to Section 9.2.2.1 of MC 90 states that the maximum amount of longitudinal tensioned steel is 4% of the total area of the section (A_c).

CEB [7] and Taerwe [33] have not mentioned any new upper limitation of the amount of steel. Therefore, the limit presented in MC 90 is maintained unchanged so far.

For concrete classes C40 to C80 and for Steel Classes S and A (steel type used in test beams) MC90 recommends in Section 5.4.3 (2) a x/d value of 0.35 to ensure sufficient ductility when a linear elastic analysis is used.

As far as HSC is concerned, CEB [7] and Taerwe [33] do not present any recommendation for the maximum value of x/d.

6.2.2 European Code EC 2 (2004)

In Section 9.2.1.1, EC 2 states that the cross-sectional area of tension reinforcement should not exceed $A_{s,max} = 0.04\ A_c$, identically as for MC 90.

In Section 5.6.3 (3) EC2 recommends that in the plastic hinge regions, the value of x/d should not exceeds 0.35 for concrete classes higher than C55/67 to ensure sufficient rotation capacity, identically as for MC 90. For NSC, EC 2 indicates 0.45 for x/d.

6.2.3 American Code ACI 318 (2005)

In the section 10.3.5, ACI 318 states that, for non prestressed flexural members, the net tensile strain in the extreme tension steel, ε_t, at nominal strength (when the strain in the extreme compression fiber reaches the assumed strain limit 0.003), shall not be less than 0.004. In section B.10.3.3, ACI 318 states that, for flexural members, the ratio of reinforcement, ρ, provided shall not exceed 0,75 of the ratio ρ_b that would produce balanced strain conditions for the section under flexure without axial load.

As far as the validity of the upper limit of the amount of reinforcement steel for HSC is concerned, nothing is mentioned by ACI committee 363 [2]. Therefore, the limit fixed for NSC should be also valid for HSC. In fact, Shah and Ahmad [25], defend that labratorial tests have confirmed that the upper limit value of 0.75 ρ_b (accepted for NSC beams) would also be adequate for HSC beams.

As far as the upper limit of the reinforcement amount is concerned, Rangan [24], recommends the equation based on the limitation of the neutral axis depth, d_n (or x), as in Australian Standard (AS 3600 [31]), (d_n not higher than 0.4d). The following equation is only valid for rectangular sections with no compressive steel bars: $\rho_{max} = 0.4\alpha\gamma f'_c/f_y$, where α and γ are the parameters corresponding to the rectangular stress block and may be determined by: $\gamma = 0.85 - 0.008\ (f'_c - 30)$ with $0.65 \le \gamma \le 0.85$ and $\alpha = 0.85 - 0.004\ (f'_c - 55)$ with $0.75 \le \alpha \le 0.85$ (f'_c in MPa). These two equations are based on New Zealand Standard (NZS 3101 [30]), assuming a constant value $\varepsilon_{cu} = 0.003$. Rangan [24], and Shah and Ahmad [25], believe that research has demonstrated that there is no reason for the variation of the ultimate strain and that the above values are satisfactory for concrete strengths up to approximately 83 MPa.

To ensure an adequate ductility in plastic region hinges, which makes redistribution of negative moments possible in design, ACI 318 recommends in Section 8.4.3 that steel strain must be $\varepsilon_s \ge 0.0075$, which correspond, for the case of maximum value of concrete strain ($\varepsilon_{cu} = 0.003$), to a x/d limit of 0.286. For each test beam, the conventional failure value of x/d was computed by considering a linear variation of the strains (see Fig. 4) and the ultimate values of $\varepsilon_{cu} = 0.003$ and $\varepsilon_{su} = 0.0075$. Comparing the x/d values of the different test beams, the values were so closed to each other that the authors decided to adopt the average value for all the beams.

ACI committee 363 [2] and Rangan [24] have not mentioned any new upper limitation for x/d.

6.2.4 Canadian Code A23.3-04 (2004)

In Section 10.5.2, A23.3-04 states that the tension reinforcement in flexural members cannot be assumed to yield unless $c/d \le 700/(700 + f_y)$ where c/d is the relative depth of the neutral axis. If c/d exceeds this limit, the failure is considered brittle. Therefore, the Canadian code only limits the c/d parameter as an alternative of the direct imposition of a maximum amount of reinforcement.

6.3 Comparison with experimental results

The maximum amount of reinforcement steel and the maximum values for x/d defined by the different codes and the proposals for future changes are compared with the results of the test beams. The aim is to investigate if the code limitations, when applied to the test beams, meet the main objective of ensuring an adequate plastic rotation/ductility.

Table 6 presents the maximum reinforcement ratio for each beam, defined either in codes of practice or proposed for future code changes. The values were computed by considering the limits fixed by the codes of practice or the corresponding proposals for alteration. These limits are directly related with the top limitation of the longitudinal reinforcement ratio in tension and were presented in the previous section. For the Canadian code, no information is presented, since the maximum amount of reinforcement is not explicitly mentioned.

From Table 6, ACI 318 and the corresponding proposal for alterations are more restrictive as far as the maximum amount of steel reinforcement is concerned. In fact, all the test beams are permitted by European requirements, but not all of them would be allowed by American requirements.

The beams that do not meet all the code requirements are the following ones: Beams A(64.1-2.21), A(63.2-2.86), A(65.1-2.86), D(85.8-3.61) and D(86.0-3.61). Rangan [24], proposal is even more restrictive and would exclude further beams: Beams C(83.6-2.69), C(83.4-2.70) and E(90.2-2.80). Typically, the excluded beams correspond to a set of beams with lower PTP (in general not higher than approximately 20%). However, some exceptions to this general remark should be pointed out.

Beam E(94.6-2.73), with a PTP of only 8.76%, should not be allowed. This beam has suffered premature failure when compared to its brother beam, Beam E(90.2-2.80) and, therefore, it shows an underestimated PTP.

Table 6, apart from the exception discussed above, shows that, when compared to European perspective, ACI Code and the proposals for alterations give a higher guaranty of an adequate plastic rotation capacity, then ductility too, for HSC beams. This is

Table 6 Upper limits for the longitudinal tensile reinforcement ratio (ρ_{max})

Beam	PTP (%)	ρ (%)	ρ_{max} (%)					
			MC 90 [9]	CEB [7]	EC 2 [10]	ACI 318 [1]	ACI 363 [2]	Rangan [24]
A(62.9-1.52) [17]	29.10	1.52	4.54	4.54	4.54	2.23	2.23	2.25
A(64.9-2.04) [17]	20.96	2.04	4.56	4.56	4.56	2.14	2.14	2.19
A(64.1-2.21) [17]	21.08	2.21	4.56	4.56	4.56	2.13	2.13	2.19
A(63.2-2.86) [17]	8.24	2.86	4.62	4.62	4.62	2.00	2.00	2.09
A(65.1-2.86) [17]	4.12	2.86	4.62	4.62	4.62	2.03	2.03	2.11
B(79.2-1.59)	29.54	1.59	4.46	4.46	4.46	2.84	2.84	2.67
B(78.9-2.09)	18.88	2.09	4.46	4.46	4.46	2.68	2.68	2.57
B(78.5-2.16)	19.18	2.16	4.46	4.46	4.46	2.66	2.66	2.56
C(82.9-2.11) [17]	21.52	2.11	4.46	4.46	4.46	2.83	2.83	2.66
C(83.9-2.16) [17]	23.66	2.16	4.46	4.46	4.46	2.87	2.87	2.68
C(83.6-2.69) [17]	18.56	2.69	4.52	4.52	4.52	2.71	2.71	2.58
C(83.4-2.70) [17]	19.36	2.70	4.51	4.51	4.51	2.70	2.70	2.58
D(88.0-1.36)	25.68	1.36	4.37	4.37	4.37	2.87	2.87	2.67
D(85.8-3.61)	16.42	3.61	4.54	4.54	4.54	2.80	2.80	2.64
D(86.0-3.61)	14.84	3.61	4.54	4.54	4.54	2.81	2.81	2.64
E(94.6-2.73)	8.76	2.73	4.52	4.52	4.52	3.11	3.11	2.87
E(90.2-2.80)	14.36	2.80	4.52	4.52	4.52	2.95	2.95	2.72
F(100.3-1.96)	26.32	1.96	4.57	4.57	4.57	3.51	3.51	3.18
F(105.2-2.66)	21.58	2.66	4.62	4.62	4.62	3.50	3.50	3.23

because ACI Code and the proposals for alterations allow lower values of the maximum reinforcement ratio. Such higher guaranty may be due to the more specific equations for the calculation of the maximum reinforcement ratio. For instance, the direct or indirect inclusion of the amount of reinforcement relative to concrete strength is an improvement, since this parameter governs the flexural behaviour of the beams. In MC 90 and EC 2, the maximum reinforcement ratio is only fixed by means of a constant percentage of the cross section area, regardless of the concrete strength. In fact, the behaviour of a beam in flexure is governed by the mechanical percentage of steel ($\rho f_y/f_c$), and not by the geometric percentage of steel (ρ). If $\rho f_y/f_c$ is sufficiently small, the strain reached by the steel reinforcement exceeds the yield strength before the concrete reaches its ultimate value at the most compressed fibre. This situation corresponds to great deformations of the member, with warning signs of imminent failure, and therefore, the member will have a ductile behaviour. Conversely, if $\rho f_y/f_c$ is high, the member will have a fragile failure.

Figures 21–26 present the evolution of PTP as a function of the longitudinal steel reinforcement ratio, not taken into account the concrete strengths. On the graphs, the limits obtained for the maximum reinforcement ratio values are also marked. The figures show the visual representation of the values presented in Table 6.

Table 7 presents the maximum value of the relative height of the compressed concrete area $(x/d)_{max}$ for each beam, defined in each codes of practice. Table 7 also includes the values of x/d at the critical section of the tested beams when they reach the failure. It was assumed that the beam's critical section reaches the failure when the maximum strain of concrete reaches ultimate value ε_{cu} or when the extension of the tensile reinforcement reaches ultimate value ε_{su}. For ε_{cu} and ε_{su} conventional values were considered because it is difficult to obtain experimental values. The conventional values of ε_{su} depend on the code that is being used. For the steel, ε_{su} value of 0.010 is normally considered acceptable for the linear/horizontal type of diagram. Some codes do not present a limit for this value. The authors found that the two options (to have or not to have a top limit for the steel strain) lead to similar results. In particular for the test beams reported here, the results are exactly the same, since the beam failure is due to concrete failure. While A23.3-04 give a constant value for ε_{cu} of 0.0035, ACI 318 presents a constant value of 0.0030, independently of the concrete strength. EC2 indicates that ε_{cu} depends on the concrete strength: $\varepsilon_{cu} = 2.6 + 35 \times [(90 - f_{ck})/100]^4$ for concrete classes $f_{ck} \geq 50$ MPa. MC 90 indicates that $\varepsilon_{cu} = 0.0035 \times (50/f_{ck})$ for 50 MPa $< f_{ck} \leq 80$ MPa. In the absence of ε_{cu} values for $f_{ck} > 80$ MPa, the value of ε_{cu} for 80 MPa was assumed to be constant for $f_{ck} > 80$ MPa.

These differences will lead to x/d values slightly different from each other when different codes of practice are used.

The values of x/d were calculated according to the experimental diagrams of the strains taken along the beam's height of the critical sections. The strains

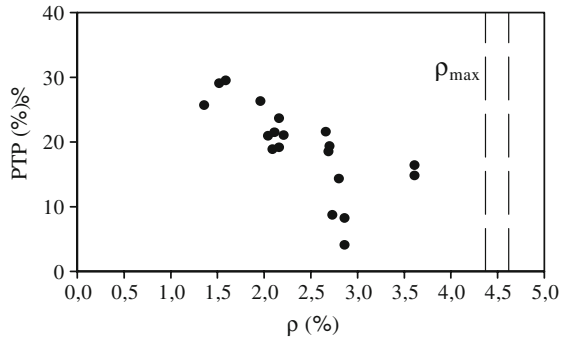

Fig. 22 Range of values for ρ_{max} (CEB [7])

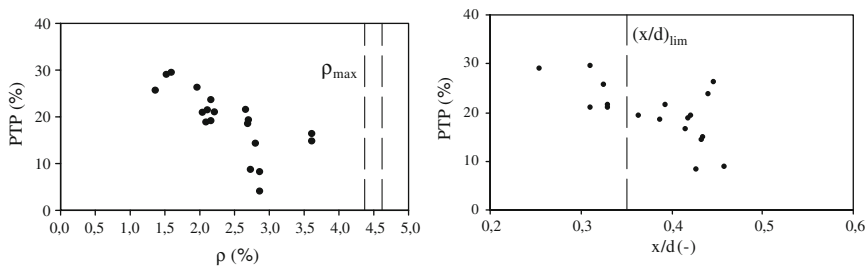

Fig. 21 Range of values for ρ_{max} and $(x/d)_{lim}$ (MC 90 [9])

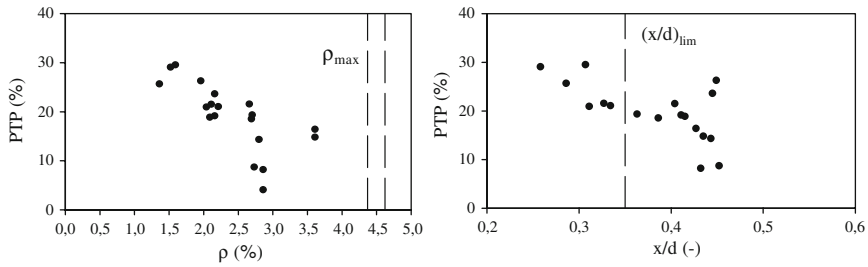

Fig. 23 Range of values for ρ_{max} and $(x/d)_{lim}$ (EC 2 [10])

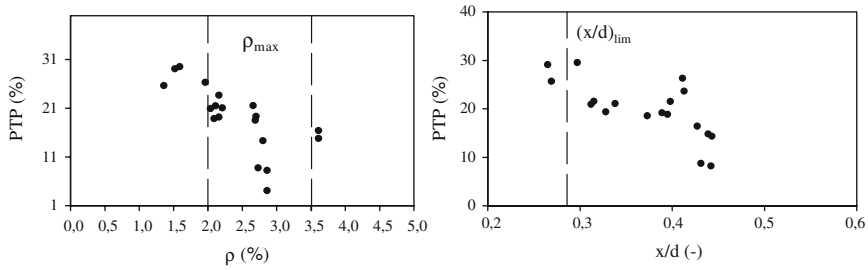

Fig. 24 Range of values for ρ_{max} and $(x/d)_{lim}$ (ACI 318 [1])

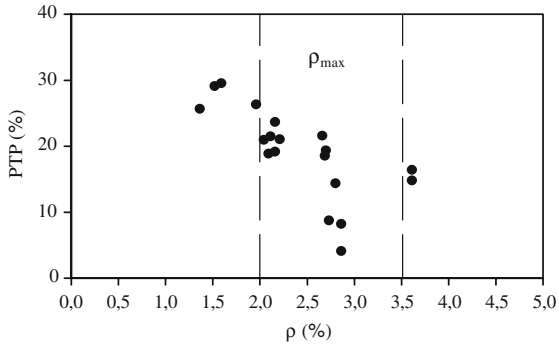

Fig. 25 Range of values for ρ_{max} (ACI 363 [2])

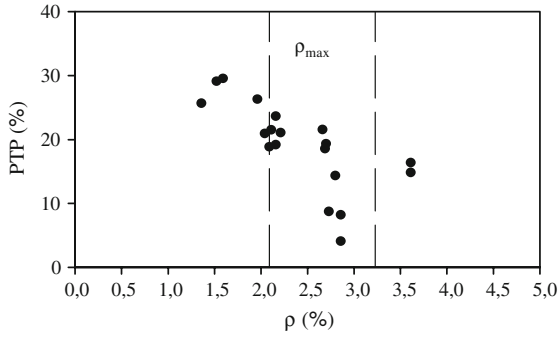

Fig. 26 Range of values for ρ_{max} (Rangan [24])

were calculated from comparing, at each load increment, the distance between pairs of Demec targets stuck on the concrete surface (see Fig. 2).

Figures 21, 23, 24, 27 also present the evolution of PTP as a function of the relative height of the compressed concrete area x/d, without take into account the concrete strengths. On the graphs, the limits obtained for the maximum x/d values are also marked.

The figures mentioned before show that, in spite of some scatter of the x/d values, it is still possible to see a decrease of the plastic rotation capacity (expressed by PTP parameter) as the relative depth of neutral axis increases. This conclusion is valid regardless of the code of practice. Therefore, the experimental results confirm the typical rule presented by the codes for NSC that consists of imposing a maximum value of x/d parameter. As expected, this rule is also valid for HSC.

This trend was already reported by the authors in a previous study where they analysed the ductility by using ductility indexes [5].

Figures 21, 23, 24, 27 also show that the limitations of x/d values presented by ACI 318, EC 2 and MC 90 when applied to the test beams, and particularly those from ACI 318 (the most restrictive of the three codes), lead to rotation capacity levels that might be considered acceptable (normally PTP values above 20%).

In contrast with the good results from the three codes mentioned above, the results from A23.3-04 are less good. In fact, as far as x/d value is concerned, this code is rather permissive and all the beams of this

Table 7 Upper limits for the relative height of the compressed concrete area

Beam	PTP (%)	MC 90 [9]		EC 2 [10]		ACI 318 [1]		A23.3-04 [11]	
		x/d (–)	$(x/d)_{max}$ (–)	x/d (–)	$(x/d)_{max}$ (–)	x/d (–)	$(x/d)_{max}$ (–)	x/d (–)	$(x/d)_{max}$ (–)
A(62.9-1.52) [17]	29.10	0.255	0.35	0.258	0.35	0.265	0.286	0.241	0.556
A(64.9-2.04) [17]	20.96	0.310		0.311		0.312		0.297	
A(64.1-2.21) [17]	21.08	0.330		0.334		0.338		0.314	
A(63.2-2.86) [17]	8.24	0.427		0.432		0.442		0.397	
A(65.1-2.86) [17]	4.12	–		–		–		–	
B(79.2-1.59)	29.54	0.311		0.307		0.297		0.283	
B(78.9-2.09)	18.88	0.419		0.415		0.395		0.372	
B(78.5-2.16)	19.18	0.421		0.411		0.389		0.257	
C(82.9-2.11) [17]	21.52	0.393		0.404		0.398		0.379	
C(83.9-2.16) [17]	23.66	0.441		0.445		0.413		0.374	
C(83.6-2.69) [17]	18.56	0.388		0.386		0.373		0.343	
C(83.4-2.70) [17]	19.36	0.364		0.363		0.328		0.302	
D(88.0-1.36)	25.68	0.326		0.286		0.269		0.249	
D(85.8-3.61)	16.42	0.416		0.427		0.427		0.430	
D(86.0-3.61)	14.84	0.434		0.435		0.439		0.413	
E(94.6-2.73)	8.76	0.459		0.452		0.431		0.393	
E(90.2-2.80)	14.36	0.433		0.443		0.443		0.418	
F(100.3-1.96)	26.32	0.447		0.449		0.411		0.364	
F(105.2-2.66)	21.58	0.330		0.327		0.315		0.298	

(–) Not available

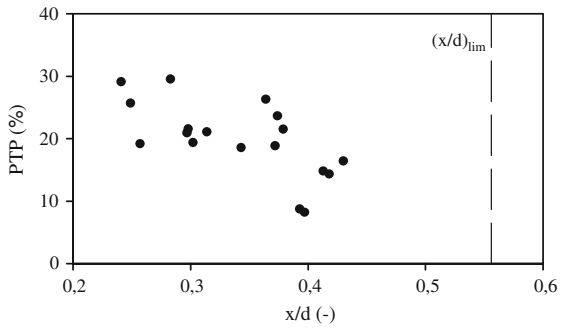

Fig. 27 Range of values for $(x/d)_{lim}$ (A23.3-04 [11])

research programme would pass the limitation indicated by this code. Some of them correspond to very low PTP values, which mean low ductility.

7 Conclusions

The θ–δ graphs presented in this paper show that after the yielding of the reinforcement steel, the beams drift from the theoretical elastic behaviour and they start to approach the theoretical plastic analysis. This approaching is coincident with the formation and development of a local plastic hinge. During a certain range of deformations, the beams approach the plastic behaviour as the load increases. Since the beam has a long distance to go from the elastic behaviour to the full plastic behaviour, it is very difficult for them to reach the full plastic behaviour. Some of them suffer just a small deviation from the theoretical elastic theory, whereas others reach values close to the full plastic behaviour. These different behaviours reflect the differences on the plastic rotation capacity of the beams. As for NSC beams, HSC beams can also reach very satisfactory values of rotation capacity (and ductility).

The parameter used in this work to evaluate the plastic rotation capacity of the tested beams (PTP) was found to be very useful since it gives very different values and facilitates the comparisons between different beams. The analysis and conclusions based on this parameter confirm, in general, the tendencies observed in previous investigation works.

It showed that the tensile reinforcement ratio is the most influent parameter as far as the rotation capacity of beams is concerned. This conclusion is confirmed by previous studies where the analysis was carried out by using ductility indexes to evaluate the ductile behaviour of the beams and by other previous studies by the authors. All these experimental studies indicate that, for constant (or approximately constant) values of the strength of concrete, the rotation capacity and the ductility decreases significantly as the tensile reinforcement ration increases, up to a certain value of this ratio. From this value of the reinforcement ratio, the rotation capacity and the ductility maintain values approximately constant. In this work, such values of the reinforcement ratio seems to be slightly above $\rho \approx 3.0\%$ or $\rho/\rho_b \approx 0.7$.

The compressive strength of concrete seems to have a small influence on the rotation capacity of the beams. Nevertheless, the authors found that for a given amount of longitudinal steel there was a slight increase of the rotation capacity with the strength of concrete. This increase seems to be a more pronounced for higher levels of reinforcement ratios.

These conclusions confirm the principal conclusions obtained in previous studies, including previous studies of the authors.

When comparing the limitations to the amount of the longitudinal tensile steel reinforcement in different codes, American code and the proposals for alterations are more restricted than the European and Canadian codes, as well as the published proposals for codes changes. Consequently, ACI Code requirements ensure more plastic rotation capacity as well as ductility for HSC beams.

The tests of HSC beams reported here indicate that the practical rule of limiting the relative height of the compressed concrete area, on critical sections, to assure adequate ductility levels, is also valid for HSC beams.

When comparing the limitations to the relative height of the compressed concrete area in different codes for a linear elastic analysis, ACI 318-05 is more restrictive than the European codes. In spite of that, ACI Code and European code requirements ensure good level of plastic rotation capacity as well as ductility for HSC beams. In this way, Canadian code is too permissive.

Current study indicates that existing provisions for x/d, of the European and American codes, for NSC are also suitable for HSC.

References

1. ACI Committee 318 (2005) Building code requirements for structural concrete, (ACI 318-05) and commentary (ACI 318R-05). American Concrete Institute, Detroit, MI
2. ACI Committee 363 (1984) State-of-the-art report on high-strength concrete. ACI Struct J 81:364–411
3. Ahmad SH, Barker R (1991) Flexural behaviour of reinforced high-strength lightweight concrete beams. ACI Struct J 88(1):69–77
4. Bernardo LFA, Lopes SMR (2003) Flexural ductility of HSC beams. Struct Concrete J Fib 4(3):135–154
5. Bernardo LFA, Lopes SMR (2004) Neutral axis depth versus flexural ductility in high-strength concrete beams. J Struct Eng 130(3):452–459
6. Carmo RNF, Lopes SMR (2005) Ductility and linear analysis with moment redistribution in reinforced high strength concrete beams. Can J Civil Eng 32(1):194–203
7. CEB (1995) High performance concrete. Bulletin d'Information no. 228
8. CEB (1998) Ductility of reinforced concrete structures. Bulletin d'Information no. 242, May 1998
9. CEB-FIP (1990) Model Code 1990. Lausanne, Suisse
10. CEN, EN 1992-1-1 (2004) Eurocode 2: design of concrete structures – part 1.1: general rules and rules for buildings. European Committee for Standardization, Brussels
11. CSA (2004) A23.3-04, Design of concrete structures. Canadian Standards Association, Ontario
12. Dahl KKB (1992) Uniaxial stress–strain curve for normal and high strength concrete. Report no. 182. Department of Structural Engineering, Technical University of Denmark, 58 pp
13. Hansen EA, Tomaszewicz A (1990) Effect of confinement on the ductility of structural members with high strength concrete. SINTEF report STF65 F90071, Trondheim, pp 184–191
14. Ko MY, Kim SW, Kim JK (2001) Experimental study on the plastic rotation capacity of reinforced high strength concrete beams. Mater Struct 34:302–311
15. Lambotte H, Taerwe L (1990) Deflection and cracking of HSC beams and slabs. ACI special publication 121, paper no. 7, November 1990
16. Leslie KE, Rajagopalan KS, Everard NJ (1976) Flexural behaviour of HSC beams. ACI J 73(9):517–521
17. Lopes SMR, Bernardo LFA (2003) Plastic rotation capacity of HSC beams. Mater Struct/Matér Construct 36:22–31
18. Mendis P (2003) Design of high-strength concrete members: state-of-the-art. Progr Struct Eng Mech J 5(1):1–15
19. Naaman AE, Harajli MH, Wight JK (1986) Analysis of ductility in partially prestressed concrete flexural members. PCI J 31(3):64–87
20. Pam HJ, Kwan A, Islam MS (2001) Flexural strength and ductility of reinforced normal and high strength concrete beams. Proc Inst Civil Eng Struct Build 146(4):381–389
21. Pastor JA, Nilson AH, Slate FO (1984) Behaviour of high-strength concrete beams. Research report 84-3. Department of Structural Engineering, Cornell University, Ithaca, New York, 311 pp

22. Paultre P, Mitchell D (2003) Code provisions for high-strength concrete – an international perspective. Concrete Int Mag Am Concrete Inst 25(5):76–90
23. Pecce M, Fabbrocino G (1999) Plastic rotation capacity of beams in normal and high-performance concrete. ACI Struct J 96(2):290–296
24. Rangan BV (1998) High-performance high-strength concrete, design recommendations. Concrete Int 20(11):63–68
25. Shah SP, Ahmad SH (1994) High performance concretes and applications. Edward Arnold, England
26. Shehata IAEM, Shehata LCD (1996) Ductility of high strength concrete beams in flexure. In: 4th international symposium on utilization of high-strength/high-performance concrete, Paris, pp 945–953
27. Shin S-W (1986) Flexural behaviour including ductility of ultra-HSC members. Ph.D. thesis, University of Illinois at Chicago, Chicago, IL, 232 pp
28. Shin S-W, Ghosh SK, Moreno J (1989) Flexural ductility of ultra-HSC members. ACI J Proc 86(4):394–400
29. Shin S-W, Kamara M, Ghosh SK (1990) Flexural ductility, strength prediction, and hysteretic behaviour of ultra-HSC members. In: Hester WT (ed) Second international symposium, SP 121-13, HSC, ACI
30. Standards Association of New Zealand (1995) Concrete structures NZS 3101 – part 1: design
31. Standards Australia (1994) Australian standards for concrete structures AS 3600, Sydney
32. Taerwe L (1991) Brittleness versus ductility of high strength concrete. Struct Eng Int 4:41–45
33. Taerwe L (1996) Codes and regulations. In: 4th international symposium on utilization of high-strength/high-performance concrete, Paris, pp 93–99
34. Tognon G, Ursella P, Coppeti G (1980) Design and properties of concretes with strength over 1500 kgf/cm^2. ACI J Proc 77(3):171–178